

# ADDITIVE MANUFACTURING OF A SINGLE CRYSTAL NICKEL-BASED SUPERALLOY USING SELECTIVE ELECTRON BEAM MELTING

SHUBHAM CHANDRA, XIPENG TAN, CHENGCHENG WANG,  
YI HONG YIP, GERALD SEET and SHU BENG TOR

*Singapore Centre for 3D Printing, School of Mechanical & Aerospace Engineering, Nanyang Technological University, 50 Nanyang Avenue, Singapore 639798*

**ABSTRACT:** Single crystal (SX) nickel-based superalloy blade forms a key element of high-temperature gas turbines that are vital to aviation and power industries, owing to its excellent creep properties at elevated temperatures. Conventional manufacturing of SX Ni-based superalloy components is a tedious and expensive process due to stringent tolerance on part geometry and SX quality. Additive manufacturing (AM) provides unique features such as economic sustainability, automated manufacturing process and capability of printing identical parts. Moreover, the future of AM technologies shows significant promise towards achieving complete layer-wise control, in terms of varying process parameters. This study employs selective electron beam melting (SEBM), a powder-bed metal AM technique, to additively manufacture a first-generation Nickel-based SX superalloy. High vacuum environment and nearly unidirectional thermal gradient, inherent with SEBM, make it the most promising AM technique for SX superalloy manufacturing. Detailed microstructural characterization using optical microscopy, scanning electron microscopy and X-ray diffraction reveal that dominant columnar grains aligned with the build direction were formed into a strongly textured superalloy sample. However, there are still some cracks occurred along the columnar grain boundaries. The correlation between SEBM processing and microstructure is discussed.

**KEYWORDS:** Additive manufacturing, Superalloys, Single Crystal, Electron Beam Melting

## INTRODUCTION

Ni-based single crystal (SX) superalloys were derived from their polycrystalline ancestors in the early 1980's by suppression of grain boundary strengthening elements like carbon, boron, zirconium and hafnium. In addition to this, large amounts of refractory elements like tungsten, tantalum and molybdenum became an integral part of the superalloys; improving their high-temperature creep properties and making them vital to the aerospace and power industry as high-pressure gas turbine components (Boyer et al. (2015)).

The conventional manufacturing of Ni-based SX superalloy blades for gas turbine applications involves either crystal seeding, or crystal selection method implemented in conjecture with various directional solidification techniques (Reed. (2008), Kubiak et al. (2016)) – a process simple in theory but similarly complex in its implementation. Process-inherent defects, such as – stray grain formation, grain misorientation and high angle grain boundaries (formed during heat treatment (Cox et al. (2003), Kobryn & Semiatin (2001))), and stringent tolerance requirements contribute to overall

cost of the manufacturing SX turbine blades thus decreasing the yield and increasing the lead manufacturing time.

Aside from the well-documented advantages of metal additive manufacturing (AM) techniques (Baufeld et al. (2010), Tan et al. (2015), Chandra & Rao (2017)), selective electron beam melting (SEBM) provides added benefit of higher energy efficiency and residual stress-free as-built specimens (Gibson et al. (2010), Chua & Leong (2014)). The application of SEBM in SX superalloy manufacturing (Ramsperger & Körner (2016) has been preliminarily achieved with a technical SX CMSX4 superalloy. However, the large build height (~20mm) required for transition to SX from a polycrystal (PX) grain growth still leaves a void in terms of achieving complete grain control.

This work is focused on AM feasibility study for a Ni-based SX superalloy – AM1 (Tan et al. (2014), Tan et al. (2014)) using SEBM technique. Effects of the process parameters on powder-bed sintering and its subsequent melting formed the major focus during this work. Detailed microstructure characterization, using optical microscopy, scanning electron microscopy and X-ray diffraction, reveals formation of largely columnar grains aligned with the build direction and presence of  $\gamma'$  precipitates distributed within the  $\gamma$  matrix. The experimental results also reveal periodic cracks formed along some of the columnar grain boundaries.

## EXPERIMENTS

An EBM A2XX (Arcam EBM, Sweden) system as shown in Figure 1 was utilized for fabrication of the superalloy samples. A tungsten filament is heated up to generate free electrons. These electrons are then accelerated towards a hollow anode by application of an accelerating voltage of 60 kV. The accelerated beam then passes through a series of electromagnetic lenses which control beam spot diameter and deflection.

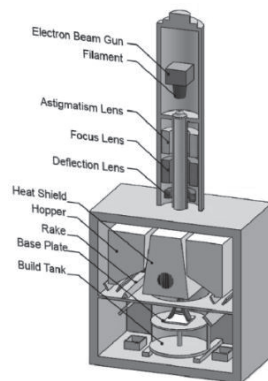


Figure 1. Schematic of an SEBM system

The powder-bed is first sintered and subsequently melted according to the cross-section of the build file and then the build platform moves down by a layer height of 50 $\mu$ m. The sintering parameters were provided to maintain a surface temperature of ~950°C. Pre-alloyed AM1 superalloy powder was utilized having a powder size distribution of 20-80  $\mu$ m with an avg. size ~50  $\mu$ m, shown in Figure 2.

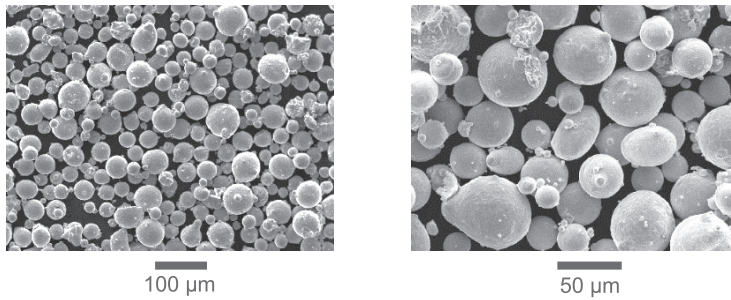


Figure 2. SEM images of AM1 superalloy powder.

For the sintering step of SEBM fabrication for AM1 superalloy powder, a beam speed of 16000 mm/s and focus offset value of 90 mA were utilized with a high average current of 31 mA to ensure a uniform build temperature of ~950°C. Optimum process parameters for the melting stage was determined by design of experiment (DoE) analysis with independent parameters of speed function (SF) and focus offset (FO). A SF value of 90 and FO values ranging from 5 to 13 were utilized to fabricate square shaped samples with dimensions  $30 \times 30 \times 3 \text{ mm}^3$  along x-, y- and z-directions respectively. The short build height proved sufficient for the feasibility study and observing the columnar grain growth trend in the superalloy samples while proving economically viable.

Standard sample preparation using electrical discharge machining (EDM) and subsequent polishing was carried out for analysis of unetched as-built surface using stereo microscopy. Etching of the samples was carried out using Marble's Reagent (10 gms  $\text{CuSO}_4$ , 50 ml HCl, 50 ml  $\text{H}_2\text{O}$ ) for grain structure analysis using scanning electron microscopy (SEM) and Kalling's No. 2 Reagent (5 gms  $\text{CuCl}_2$ , 100 ml HCl, 100 ml  $\text{CH}_3\text{CH}_2\text{OH}$ ) for revealing the  $\gamma/\gamma'$  microstructure using field emission scanning electron microscopy (FESEM). Bulk phase analysis using X-ray diffraction (XRD) provides qualitative information about the strongest texture in the as-built superalloy samples.

## RESULTS

### Microstructure Characterization

Figure 3 shows micrographs of polished, unetched cross-sections observed under a stereomicroscope. The micrographs show cracks aligned with the build direction and distributed uniformly across the cubical structure. As seen in the transverse cross-section micrograph, the cracks originate with in few layers from the start plate and propogate all the way to the top surface of the sample.

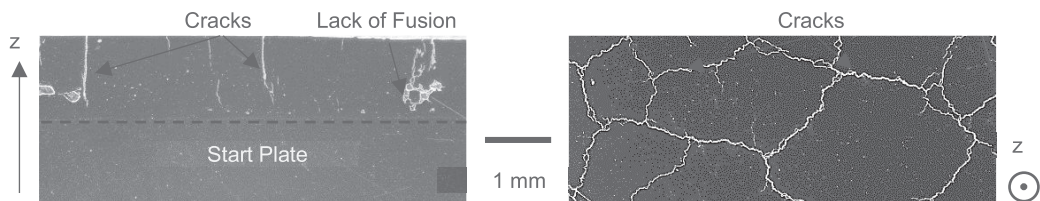


Figure 3. Low magnification images of elevation and plan views showcasing crack distribution.

Figure 4 shows the microstructure on the longitudinal section under SEM, revealing highly columnar grains aligned with the build direction with cracks mainly occurring at their grain boundaries. ImageJ, an open source image processing tool was used to measure the primary dendrite arm spacing (PDAS) from the SEM images. A PDAS value of  $3 \pm 0.5 \mu\text{m}$  was recorded near the top surface (Figure 4(d)). Figure 5 shows micrograph of the xy cross section, etched using Kalling's No. 2 reagent observed under FESEM. The micrograph shows intermediate distribution of  $\gamma'$  precipitates with coarse precipitates near the grain boundary. The XRD analysis shows strong  $\langle 001 \rangle$ -texture aligned with the build direction (Figure 6).

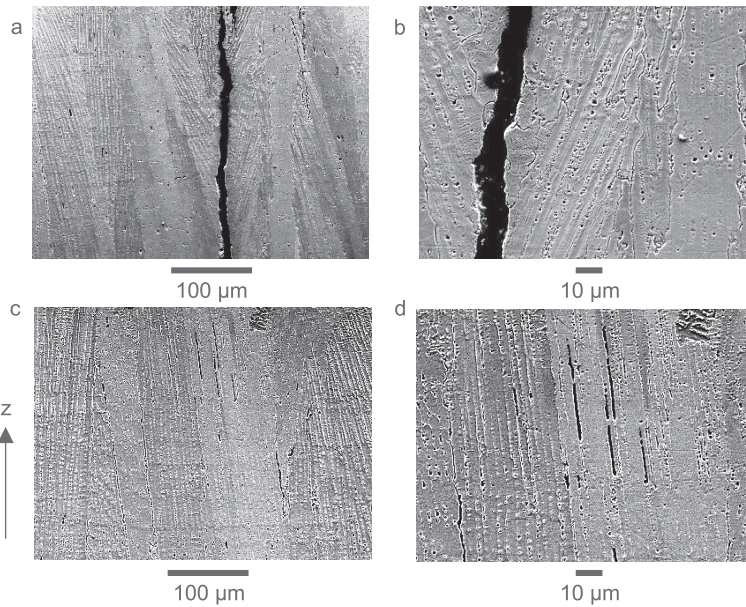


Figure 4. SEM images of SEBM fabricated AM1 as-built samples. Scale is 50 μm

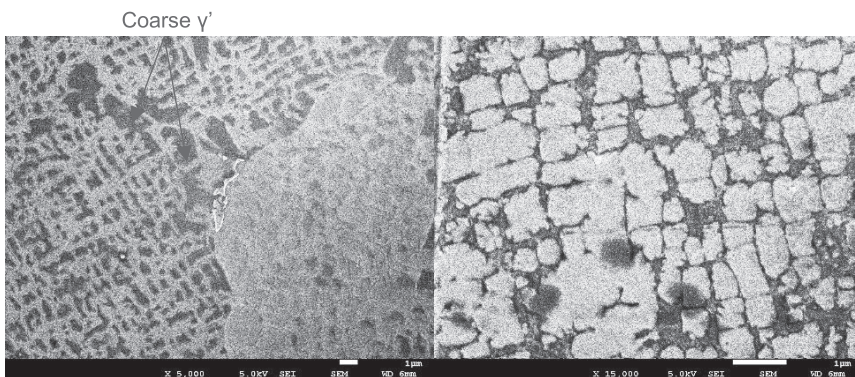


Figure 5. FESEM images showing distribution of  $\gamma'$  precipitates. The grain boundaries show presence of coarsened precipitates. Scale is 1 μm.

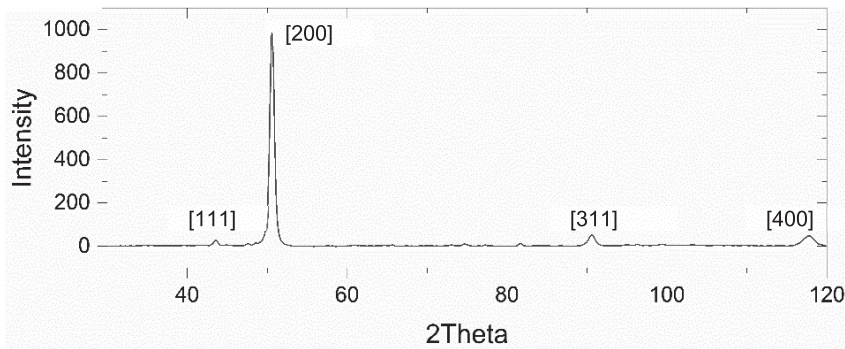


Figure 6. XRD plot for the top surface of sample

## DISCUSSION

Given the nature of crack distribution within the specimens, it is believed that these are residual stress induced cracks as reported by Ramsperger & Körner (2016). Martin et al. (2017) demonstrated that these – caused by hot tearing due to material segregation at the grain boundaries, can be eradicated by inducing columnar to equiaxed transition (CET). Inducing CET will deteriorate the cause of using SEBM for SX, hence there is a need to produce crack-free samples without compromising columnar grain structure itself. Ramsperger & Körner (2016) have demonstrated that these cracks are present only within the polycrystalline structure and once the PX to SX transition takes place, these cracks are eliminated along with the grain boundaries.

A major advantage of using SEBM for fabrication of superalloy parts is observed in terms of PDAS value of  $\sim 3 \mu\text{m}$  near the top surface. PDAS correlates directly to the time required for homogenization of alloys samples at solution annealing temperature. Ramsperger et al. (2015) managed to achieve complete homogenization of SEBM fabricated CMSX4 samples with an avg. PDAS of  $6 \mu\text{m}$  in only 4 minutes of exposure of the samples at the annealing temperature which ordinarily takes  $\sim 20$  hours for cast samples. This can provide an economic alternative to already expensive post processing of conventionally manufactured SX blades.

## CONCLUSIONS

Although AM1 is a Ni-based SX superalloy with refractory elements such as tungsten, molybdenum, chromium and cobalt, it can be successfully 3D printed with SEBM technique with substantial columnar grain growth and  $\gamma'$  precipitation. The presence of uniformly distributed cracks within the short build sample and their affinity to columnar grain boundaries shows significant promise for eradication of such cracks by crystal selection or competitive grain growth for larger build heights. The precipitation of  $\gamma'$  in the as-built samples shows new aspiration for in-situ heat treatment associated with SEBM technique.

## ACKNOWLEDGMENTS

The authors acknowledge the Singapore Centre for 3D printing and the School of MAE, Nanyang Technological University for the experimental and analytical facilities without which this research would not have been possible.

## REFERENCES

- Boyer, R., Cotton, J., Mohaghegh, M., & Schafrik, R. (2015) “Materials considerations for aerospace applications”, *MRS Bulletin*, 40(12), 1055–1066.
- Baufeld, B., Van der Biest, O., & Gault, R. (2010) “Additive manufacturing of Ti-6Al-4V components by shaped metal deposition: Microstructure and mechanical properties”, *Materials & Design*, vol. 31, 106–111.
- Chandra, S., & Rao, B. C. (2017). A study of process parameters on workpiece anisotropy in the laser engineered net shaping (LENS<sup>TM</sup>) process. *Journal of Physics D: Applied Physics*, 50(22), 225303.
- Chua, C. K., & Leong, K. F. (2014) 3D PRINTING AND ADDITIVE MANUFACTURING: Principles and Applications (with Companion Media Pack) of Rapid Prototyping. *World Scientific Publishing Co Inc*.
- Cox, D. C., Roebuck, B., Rae, C. M. F., and Reed, R. C. (2003) “Recrystallisation of single crystal superalloy CMSX-4”, *Materials Science and Technology*, 19(4), 440–446.
- Gibson, I., Rosen, D. W., & Stucker, B. (2010) “Additive manufacturing technologies”. *Springer*, vol. 238.
- Kubiak, K., Szeliga, D., Sieniawski, J., and Onyszko, A. (2015) “The unidirectional crystallization of metals and alloys (turbine blades)”, *Handbook of Crystal Growth (2<sup>nd</sup> Ed.)*, Elsevier, 413–457.
- Martin, J. H., Yahata, B. D., Hundley, J. M., Mayer, J. A., Schaedler, T. A., & Pollock, T. M. (2017). 3D printing of high-strength aluminium alloys. *Nature*, 549(7672), 365.
- Ramsperger, M., Mújica Roncery, L., Lopez- Galilea, I., Singer, R. F., Theisen, W., & Körner, C. (2015). Solution Heat Treatment of the Single Crystal Nickel- Base Superalloy CMSX- 4 Fabricated by Selective Electron Beam Melting. *Advanced Engineering Materials*, 17(10), 1486-1493.
- Reed, R. C. (2008) “The superalloys: fundamentals and applications”, *Cambridge university press*.
- Tan, X. P., Mangelinck, D., Perrin-Pellegrino, C., Rougier, L., Gandin, C. A., Jacot, A., ... & Jaquet, V. (2014). Atom probe tomography of secondary  $\gamma'$  precipitation in a single crystal Ni-based superalloy after isothermal aging at 1100° C. *Journal of Alloys and Compounds*, 611, 389-394.
- Tan, X. P., Mangelinck, D., Perrin-Pellegrino, C., Rougier, L., Gandin, C. A., Jacot, A., ... & Jaquet, V. (2014). Spinodal decomposition mechanism of  $\gamma'$  precipitation in a single crystal ni-based superalloy. *Metallurgical and Materials Transactions A*, 45(11), 4725-4730.
- Tan, X., Kok, Y., Tan, Y. J., Descoins, M., Mangelinck, D., Tor, S. B., Leong, K. F., & Chua, C. K. (2015) “Graded microstructure and mechanical properties of additive manufactured ti-6al-4v via electron beam melting”, *Acta Materialia*, 97, 1–16.